

Estimating Chlorophyll Content and Bathymetry of Lake Tahoe Using AVIRIS Data

Michael K. Hamilton, Curtiss O. Davis, W. Joseph Rhea, and Stuart H. Pilon

Jet Propulsion Laboratory, California Institute of Technology, Pasadena

Kendall L. Carder

Department of Marine Science, University of South Florida, St. Petersburg

An AVIRIS image was obtained at Lake Tahoe on 9 August 1990, along with in situ data. Profiles of percent transmission of monochromatic light, stimulated chlorophyll fluorescence, photosynthetically available radiation, and spectral upwelling and downwelling irradiance, and upwelling radiance were measured. Chlorophyll-a + phaeopigments, total particulate absorption, detritus absorption, and absorption due to colored dissolved organic matter were measured on discrete samples. Spectral reflectance at the surface was measured with a handheld spectroradiometer. Image pre-processing included increasing the instrument signal-to-noise ratio by filtering to reduce patterned noise and spatial resampling, and application of LOWTRAN-7 as an atmospheric correction. Several analyses were then performed illustrating the utility of the AVIRIS over a dark water scene. The water-leaving radiance measured by the AVIRIS compares very well with the upwelling radiance measured in-water, everywhere but in the very short wavelength channels. After recalibrating one

AVIRIS channel, the chlorophyll concentration derived from the image compares extremely well with that measured with bottle samples. Application of the pigment algorithm to the rest of the lake was confounded by covarying absorption at 440 nm by colored dissolved organic matter (CDOM), underscoring the importance of accurate calibration of the instrument in the short-wavelength channels. Surface spectroradiometer measurements made along a transect of varying depth were used to condition a multiple linear regression bathymetry model. By applying the model coefficients to a portion of the image, a bathymetry map of the shallow parts of the lake was constructed which compares favorably with published lake soundings, indicating the potential for a bottom-reflectance correction to coastal ocean color imagery.

INTRODUCTION

In preparation for future satellite-borne multi-channel imaging spectrometers planned for deployment in the coming decades, Airborne Visible/Infrared Imaging Spectrometer (AVIRIS;

Address correspondence to Michael K. Hamilton, MS 300-323, JPL, California Inst. of Technology, 4800 Oak Drive, Pasadena, CA 91109.

Received 15 February 1992; revised 31 October 1992.

Vane et al., 1993) data are being used to develop and test algorithms for high spectral and high spatial resolution color imagery. The Coastal Zone Color Scanner (CZCS) on the Nimbus-7 platform was the first satellite ocean color sensor, with four bands in the visible and one near-infrared. The CZCS greatly improved understanding of the links between physical processes, watermass variability, and productivity in the ocean before it failed in 1986. To continue mapping global and regional distributions of pigmented material in the ocean, launches are planned for the instruments SeaWiFS, MERIS, OCTS, MODIS-N, and HIRIS (Table 1), between 1993 and 2013. AVIRIS, with 220 9.5 nm spectral channels spanning 0.4–2.4 μm and 20 m pixel size, is uniquely suited for the developmental support of HIRIS, which will map surface reflectance in 192 10.5-nm spectral channels, with a spatial resolution of 30 m. AVIRIS pixels and channels can be resampled to produce unaliased simulations of virtually any of the other color instruments, and provide a testing-ground for algorithm development and verification over a wide range of geologic, atmospheric, limnologic, oceanographic, and botanical investigations.

Application of this imagery to water environments can be more complex than geologic or vegetative scenes. The AVIRIS was originally designed for land targets with 10–50% reflectance. Water targets have very low reflectances, with maximum values on the order of 2–7%. Light penetrates meters to tens of meters into the water, and multiple scattering as well as absorbing processes modify the upwelling spectrum. The presence of components with similarly shaped or over-

lapping absorption spectra confounds attempts to derive quantitative estimates of photosynthetic pigments. Also, the low reflectance of water targets necessitates greater signal-to-noise (SNR) performance from the instrument in the region of greatest interest, 0.4–0.7 μm .

Irradiance incident on the surface of the water has been modified by the approximately 700 km trip through the atmosphere through the processes of scattering by air molecules and aerosols, and by absorption by ozone, oxygen, and water. The reflection, scattering, and transmission of light across the air–water interface are governed by the Fresnel coefficients of reflection, which are in turn modified by surface roughness, a function of wind speed. Foam and bubbles also contribute to the uncertainty in the magnitude and spectral distribution of downwelling irradiance just below the surface.

Photons that do penetrate can be absorbed by water itself, pigments in photosynthetic plant material, or dissolved organic substances. Multiple scattering by both photosynthetic and non-photosynthetic particles can lead to increased probability of eventual absorption, or photons can be eventually ejected back through the surface. The magnitude and angular distribution of the scattering process are functions of the size distribution, photosynthetic character, mean shape, and concentration of suspended particulate material.

Upwelled light emerging from the surface carries information on all these processes. Because nearly all absorption takes place in the upper two to three attenuation lengths (typically no more

Table 1. Characteristics of Proposed U.S. and International Spaceborne Ocean Color Sensors

Sensor	CZCS	SeaWiFS	OCTS	MODIS	MERIS	HIRIS
Dates	1978–1986	1993–1998	1995–1998	1998–2013	1998–2003	2003–2013
Coverage	< 10% / day	Global / 2 days	Global / 2 days	Global / 2 days	Global / 3 days	Selected sites, 2-day revisit
Ocean color bands	4	8	8	9	11	10 nm full spectral
Signal-to-noise ratio	100–200	420–680	450–500	500–1200	400–500	200–360
Spatial resolution	0.8 km	1.13, 4.5 km	0.7 km	1 km	250 m, 1 km	30 m
Calibration: radiometric spectral	Partial No	Complete No	Complete No	Complete Yes	Complete Yes	Complete Yes
Reference ^a	Hovis et al. (1980)	Baker et al. (1987)	Yoder and Fukushima (1991)	Salmonson et al. (1989)	Rast and Bezy (1990)	Goetz and Davis (1991)

^a For future sensors the table has been updated with the latest information as of 21 February 1992.

than a few meters to tens of meters), this information is confined to that region, and quantities derived from the water-leaving spectral radiance are generally referred to as surface values.

To date, there are no reliable methods of linearly deconvolving or unmixing the effects of multiple absorbing species from the spectrum of upwelled light from the surface of a body of water. This in contrast to geologic work, where sharp reflectance features that are unique to certain minerals can be exploited in linear unmixing models (see Boardman and Goetz, 1991, and references therein). Possible avenues being investigated for water analyses include signal-system analysis and formation of nonlinear convolution kernels using alternative sets of basis functions, singular value decomposition (SVD) of orthogonally transformed endmember spectra, and using the derivatives and transfer functions of the upwelled spectrum

Previous investigations using AVIRIS over water targets have demonstrated the presence of correlated noise in the data and low SNR, making it difficult to estimate values for surface chlorophyll concentrations (Pilorz and Davis, 1990a; Melack and Pilorz, 1990). Subsequently, the design and engineering team has made great progress in reducing noise, to the point that the SNR ratio in the visible and near-IR is now over three times the original specifications, and the current (1992) flight season promises to be approximately 50% better than that. Further, software was developed as part of this study to remove certain types of patterned noise without significantly affecting signal.

Pilorz and Davis (1990a) point out that in order to resolve a change in chlorophyll concentration on the order of 1 mg m^{-3} , it is necessary to resolve a water-leaving radiance signal of $\sim 0.05 \mu\text{W cm}^{-2} \text{ sr}^{-1} \text{ nm}^{-1}$. For a typical water-leaving radiance of ~ 0.6 at 450 nm, this necessitates a SNR (calculated as the ratio of the mean value to the standard deviation of a homogeneous 100×100 pixel area of the image) of at least 12 for the water-only part of the signal, or 95 for the total signal (including the effects of the atmosphere) measured by the sensor ($4.7 \mu\text{W cm}^{-2} \text{ sr}^{-1} \text{ nm}^{-1}$).

In this study, an AVIRIS water scene is compared to *in situ* surface and in-water measurements. Previously published algorithms are applied to the data to estimate bathymetry in the shallow parts of the lake and concentrations of

photosynthetic pigment. The image-derived estimates are compared to both bottle samples of chlorophyll and to concentrations derived from the in-water optical measurements, and the differences discussed. Based on the bathymetry model, a scheme for correcting coastal and lake imagery for the effects of shallow bottom reflectance is suggested.

STUDY AREA

Lake Tahoe, the third largest alpine lake in the world, has an average depth of 302 m and a maximum depth of 503 m. It is located at an elevation of 1906 m in the Sierra Nevada mountains on the California–Nevada border, at 39.14° N , 120.19° W . The water is extremely clear, with near-surface chlorophyll values $< 0.2 \text{ mg m}^{-3}$. The clarity of the water is maintained by an effort by the local populace to divert sewage from surrounding areas, the size of the lake, and its closed nature, in that there are no major incoming tributaries. Lake Tahoe was chosen as a study site because of its pure water and high altitude location. The low chlorophyll values are comparable to those found in the oligotrophic central gyres of the world ocean, and as such it represents the clear-water endpoint in the range of both freshwater and oceanographic conditions. The area is easily accessible by small boat and AVIRIS flyby, and its high elevation location in clear air makes atmospheric correction less sensitive to the aerosol variability associated with marine environments.

An oligotrophic body of water such as Lake Tahoe should have low spatial variability. Low surface chlorophyll and lack of significant discharge and tributary input make the central lake waters extremely homogeneous. Variations in a subimage of the central portion of the lake are unlikely to result from phytoplankton patchiness or point sources of effluent, and would most likely have been introduced by variability in atmospheric water vapor or instrument noise.

DATA COLLECTION AND METHODS

The overflight occurred at 10:30 PDT on 9 August 1990. The plane had a heading of 110° , at a nominal altitude of 20 km. Solar zenith angle was

39.8°, and solar azimuth was 114.2°, so that the aircraft was flying nearly directly into the sun to minimize glint and uneven illumination across the scene. The surface of the lake was calm; windspeed was essentially zero at the time of the overflight.

Several stations were occupied for collection of in-water optical data with a Bio-Optical Profiling System (BOPS; Smith et al., 1984). The package is built around a Biospherical Instruments MER-1048 spectroradiometer, which measures up (eight channels) and downwelling (13 channels) spectral irradiance and upwelling radiance in eight channels. The modified package includes sensors for photosynthetically available radiation (PAR; integrated scalar irradiance between 400 nm and 700 nm), temperature, conductivity, chlorophyll fluorescence, transmission of a beam of collimated light, depth, tilt, and roll. The spectroradiometer samples all channels at 16 Hz, averages to 4 Hz, and transmits the data to a computer on deck. The data are subsequently binned to 1 m depth averages and corrected for ship shadow and other artifacts. At each station, chlorophyll and phaeopigment samples were collected and processed following the procedures of Strickland and Parsons (1972). The location of the sampling stations are on the area map (Fig. 1).

Specific absorption coefficients for particulates were obtained for surface waters and the total particulate absorption coefficients were determined, using the method of Mitchell and Kiefer (1988). Methanol-insoluble particulate and detrital pigment absorption were determined using the hot methanol extraction method (Kishino et al., 1985), as modified by Roesler et al. (1989). For lake water absorption coefficients, the samples were filtered twice, the second time through a 0.2 μm Nucleopore filter and optical densities were measured with a Cary 2000 spectrophotometer using a 10 cm quartz cuvette. Absorption through a distilled water blank was subtracted, leaving absorption by colored dissolved organic matter (CDOM) in the lake water. An empirical function was fit to these data to describe CDOM continuously as a function of wavelength greater than 0.4 μm , that is,

$$\text{abs}_{\text{CDOM}}(\lambda) = 0.027636 * \exp[-0.13 * (\lambda - 400)]. \quad (1)$$

Remote-sensing reflectance measurements were determined using the methodology described in Carder and Steward (1985) and Peacock et al.

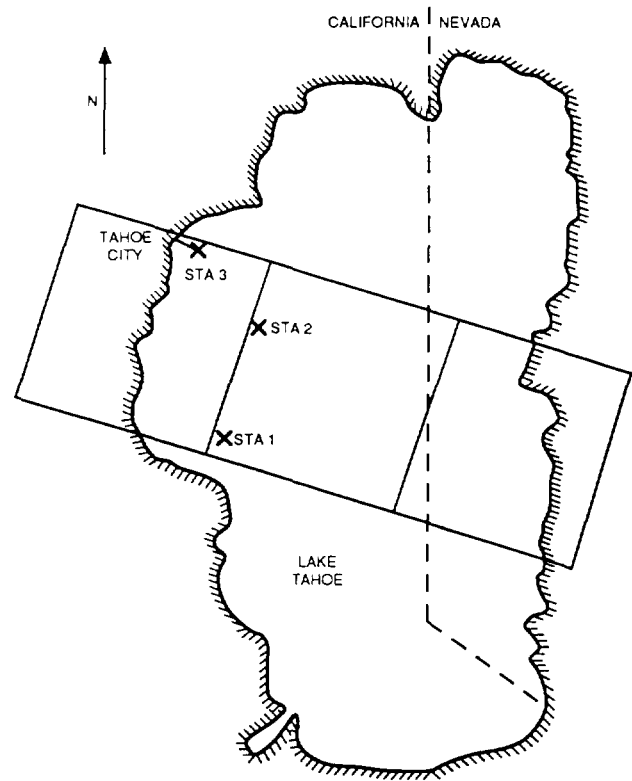


Figure 1. Location map of the Lake Tahoe area, with boundaries of the scenes collected. The in-water sampling stations are marked, as is the transect line where the reflectance spectra were collected. The *in situ* data presented in this study were collected at station 2, and the scene used for analysis is a combination of the northernmost two scenes, concatenated to produce a square (614 \times 614 pixel) image.

(1990). To improve spectral resolution to 6 nm, a 200- μm entrance slit was added to the Spectron Engineering radiometer, Model 590, and a vertical polarizer was placed in front of the slit to minimize uncertainty about the Fresnel-reflected skylight received in the upwelling radiance path. Spectralon, a NBS-traceable 10% gray diffuse reflector, was used to convert the downwelling global irradiance to upwelling radiance for measurements by the Spectron radiometer. Sequential measurements of the gray reflectance standard, water (less than 20° nadir angle), and sky (less than 20° zenith angle at the same azimuthal angle as the water measurement) were all taken in less than 15 s. Remote-sensing reflectance was derived from

$$\frac{L_w}{E_d} = \frac{[S_{w+s} - S_s * \rho(\theta)]}{(\pi * S_g / \text{refl})}, \quad (2)$$

where the S terms are for the signals from the water plus reflected skylight, from skylight, and from the gray standard, respectively; $\rho(\theta)$ is the Fresnel reflectance of seawater at the angle θ for vertically polarized light ($< 2.1\%$), and refl is the reflectivity of the gray standard. The factor of π converts reflected radiance values into irradiance values for a Lambertian diffuser. The responsivity of the radiometer is not explicitly shown, since it is a term in both the numerator and denominator of the ratio.

DATA PREPROCESSING

Signal processing and analysis of BOPS and AVIRIS data were done on a Sun SPARCstation-2, using a combination of FORTRAN programs and the Interactive Data Language (IDL; Research Systems, Inc., Boulder, Colorado). Portions of the AVIRIS data analysis were carried out using the Spectral Image Processing System (SIPS) developed at CSES/CIRES, University of Colorado, Boulder, Colorado.

Ship effects are defined as a deviation in the expected light field in the upper 10–20 m of the in-water optical profile, which cannot be correlated with any changes in the chlorophyll fluorescence or the percent beam transmission. Ship effect may include ship-shadow (light intensities less than expected) or ship reflectance (light intensity greater than expected). At stations where ship effect was identified in the upper portion of the optical profiles, that portion was replaced with an extrapolated polynomial curve, derived from the lower unaffected portion of the data. Also, the optical data in some casts were smoothed to remove intensity variations caused by wave focusing, the ship's motion, and instrument tilt and roll. Each spectral channel was corrected individually using interactive software. No corrections were made to channels that did not have clear artifacts. The success of the data correction procedure was evaluated by comparing profiles of the diffuse attenuation coefficient for downwelling irradiance (K_d) with those predicted by the model of Morel (1988), using the measured chlorophyll plus phaeopigment values.

Software was developed to locate and remove the regular noise signals in the AVIRIS data which are due to radio interference, variability in the

power supply, and insufficient cable shielding. The noise signals appear in the time sequential data as sinusoids of fairly constant frequency and mean amplitude. For these data, it was sufficient to locate the dominant noise frequencies over clear water (e.g., a portion of the scene with a uniform low signal) by FFT, and then to eliminate noise only at these frequencies over the rest of the image. This ensures that real features are not removed, of special importance in scenes containing both land and water. Sharp features within the data contribute some power over a range of spatial frequencies and at different phases. Unintentional elimination of just some of this power during cleaning will result in a "reflection" of a feature across the image. The use of two-dimensional FFTs helps to minimize this ringing, but is not sufficient in itself. It was necessary to locate sharp features with a threshold test and flag land pixels. Average water spectra were subtracted from water pixels, and an adjusted land spectrum subtracted from flagged pixels. This adjusted spectrum consisted of an average land spectrum, plus or minus some coefficient times the principle component of variation for the spectra of all flagged pixels (found by singular value decomposition).

After subtracting the land fits and mean water spectrum, an FFT was performed on the two-dimensional array, and the prescribed amount of power removed from each peak at the phase at which the peak was observed in the test area, and the inverse FFT resulted in a cleaned image. This technique increased the SNR, especially in the blue, without degrading the information contained in the image. For data sets with a subscene free of features from which to characterize the noise, the algorithm strikes a good compromise between cleaning deterministic noise without cleaning real signal. Figure 2 illustrates the utility of the filtering algorithm in increasing the SNR of some dark AVIRIS scenes collected previous to 1991. An average of 100 lines over water in the image is plotted as raw data number (DN, converted to floating point) versus cross-track pixel for Band 14, both before and after applying the filtering algorithm. Approximately 3 parts in 680, or 0.4%, of the signal was lost to the filter. Again applying detection of variability in chlorophyll concentration as a criterion for signal, a variance of 0.003 data numbers in band 14 con-

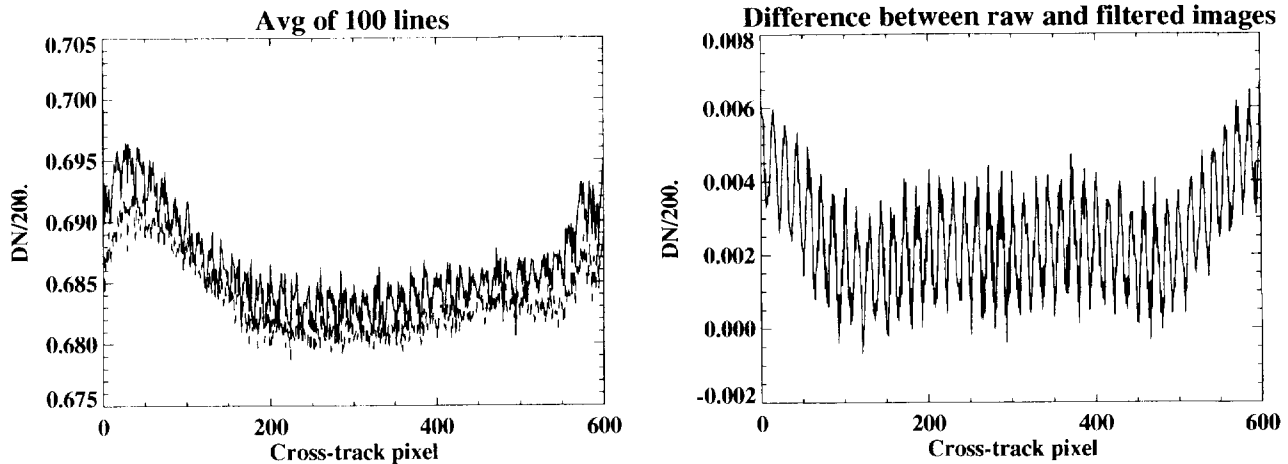


Figure 2. Average of 100 lines of data from unfiltered AVIRIS Band 14 (537 nm) over clear water, the post-filtered average of the same 100 lines, and the residual illustrating the amount of variability removed. Note the vignetting effect of the sensor, which was subsequently removed during the radiometric calibration step.

verts to approximately $0.03 \mu\text{W cm}^{-2} \text{sr}^{-1} \text{nm}^{-1}$, less than the threshold for detection of a change in 1 mg m^{-3} chlorophyll.

The cleaned image was then calibrated radiometrically and adjusted for the effects of dark current and instrument vignetting, using the calibration coefficients and auxiliary files provided by the JPL AVIRIS project. To correct for the effects of the atmosphere, the radiative transfer code LOWTRAN-7 (Kneizys et al., 1988) was used to model the path-scattered radiance expected on that day, parameterized with the observed meteorological conditions. Given the small size of the image ($12 \times 10 \text{ km}$), and the clear air in the morning at high elevation, the correction was not allowed to vary over the image; rather, one spectrum was applied to all water pixels. While this could introduce error in some circumstances, in that water vapor has been shown to vary significantly within an AVIRIS image in mountainous areas as a function of topography (Green et al., 1991), the conditions on the morning of this experiment were dry and clear, and the assumption of atmospheric spatial homogeneity over the water is a reasonable one.

LOWTRAN-7 was run in radiance mode, using a multiple-scattering midlatitude summer model with a rural aerosol profile, and a visibility of 120 km. Two separate sensor-target geometries were used, similar to the method of Carder et al. (1993), to model the reflected atmospheric skylight and path-scattered radiance. One geometry used was with the observer on the surface, looking into

space. The path radiance viewed from this configuration is skylight, 2% of which was reflected off the surface of the water and propagated back up to the aircraft using the diffuse transmission of the atmosphere, modeled from 0 to 20 km. The water-leaving radiance component of the signal received by the AVIRIS was then modeled as

$$L_w = (L_{\text{img}} - L_{\text{path}} - L_{\text{sky}}\rho t_d) / t_d, \quad (3)$$

where

- L_w = water-leaving radiance,
- L_{path} = total atmospheric path-scattered radiance,
- L_{sky} = skylight, looking up from the surface into space,
- ρ = Fresnel reflectance set equal to 2%,
- t_d = atmospheric diffuse transmission.

Figure 3 shows the amount of signal removed as atmosphere.

ANALYSIS

In-water attenuation profiles were derived as the negative logarithm of the depth-gradient of downwelling irradiance in each channel of the profiling instrument. These attenuation coefficients were used to propagate the most shallow upwelling radiance measurement to just below the surface. Studies in hydrologic optics (cf. Austin, 1974) have shown that the value of upwelled radiance

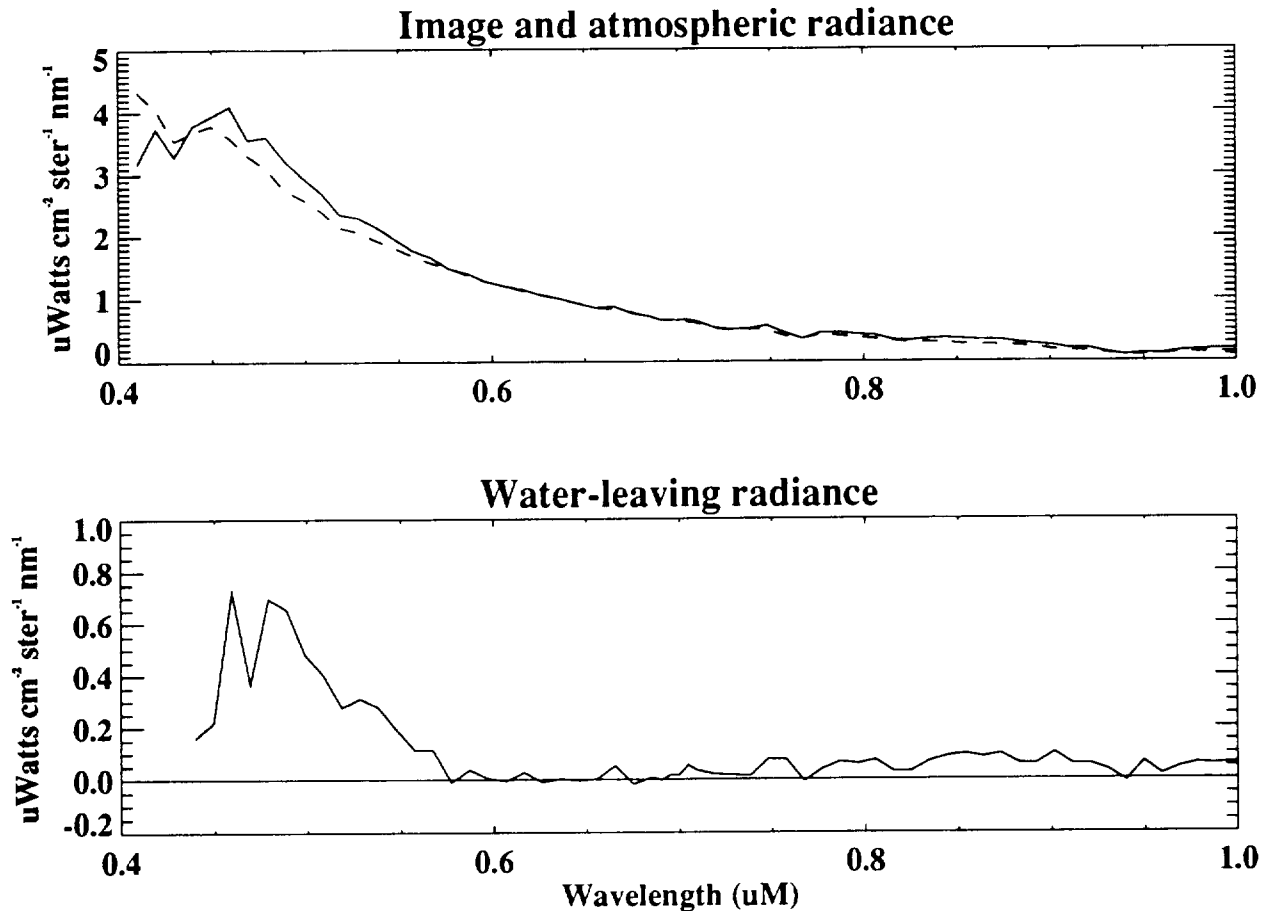


Figure 3. The raw image spectrum from station 2, the modeled atmospheric spectrum, and water-leaving radiance residual spectrum.

just above the surface is related to upwelling radiance just below the surface by an approximate factor of 0.544, which takes into account the Fresnel coefficients of reflectance and underwater diminution of the cone of light due to differences in refractive indices between air and water. The upwelling radiance just above the surface can thus be derived from in-water measurements (dropping the wavelength dependence for brevity) from the relationship (Gordon et al., 1988):

$$L_u^+ = \frac{E_d^+ (1 - \rho)(1 - \bar{\rho})R}{Qn^2}, \quad (4)$$

where E_d^+ is the downwelling irradiance above the surface, n is the refractive index of water (1.33), ρ and $\bar{\rho}$ give the Fresnel reflectance for downwelling and upwelling radiation (both set equal to 0.02 for calm waters and nadir viewing angle), and R is the diffuse reflectance just below the surface. Using the definitions

$$R = E_u^- / E_d^- \quad \text{and} \quad Q = E_u^- / L_u^-, \quad (5)$$

we arrive at the relation

$$L_u^+ = (0.96 / 1.79) E_d^+ L_u^- / E_d^-, \quad (6)$$

which agrees within a few percent of the simpler relation

$$L_u^+ = (0.98 / 1.79) L_u^-, \quad (7)$$

which was used to derive the water-leaving radiance estimates to compare with the image.

Chlorophyll concentration was estimated from the AVIRIS data for the surface waters of Lake Tahoe using the CZCS algorithm for low pigment concentration (Gordon et al., 1983),

$$\log_{10}[\text{chl}a] = 0.053 + 1.71 \log_{10}(L_w(550) / L_w(443)), \quad (8)$$

where $L_w(550)$ and $L_w(443)$ are the values of upwelled radiance from the surface in 20 nm (fwhm)

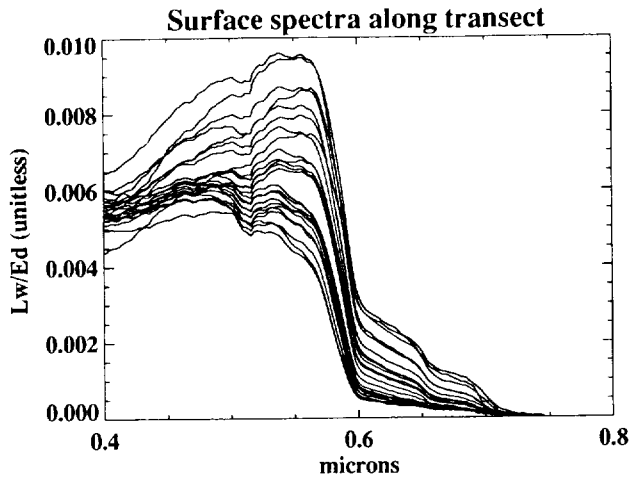


Figure 4. Surface reflectance spectra, collected along a transect over shallow water where the bottom was clearly visible. Depth along the transect varied from 10.4 m to 3.4 m (top curve).

bands centered at 550 nm and 443 nm. The CZCS bands were approximated using the mean value of the bands bracketing each of the wavelengths, that is, Bands 4 and 5 for 440 nm and Bands 16 and 17 for 548 nm, each of which are 10 nm wide. Instrument signal-to-noise ratio was increased for this analysis using a combination of the previously described filter algorithm, and by generating 1.13 km pixels using the proposed spatial response of the SeaWiFS sensor.

The relationship between remotely-sensed radiance, bottom reflectance and water depth was investigated using 25 surface spectra collected with the Spectron, along a transect where the bottom was clearly visible (the transect line is from station 3 to the shore in Fig. 1). The length of the transect was ca. 1 km, and water depth ranged from 10.4 m to 3.4 m. Using the results

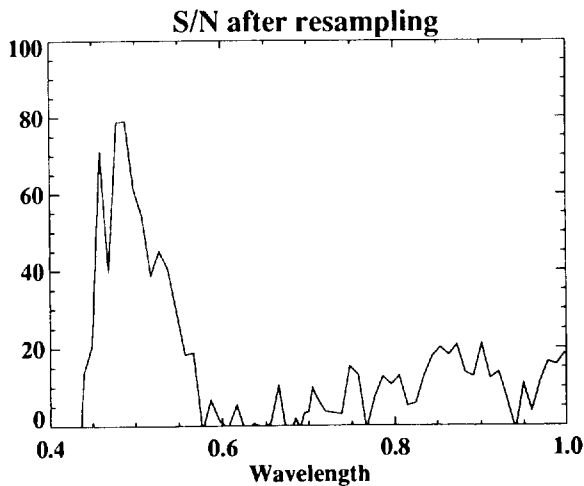
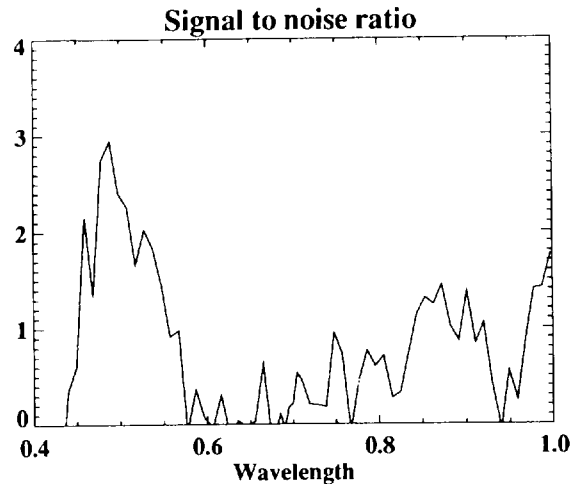
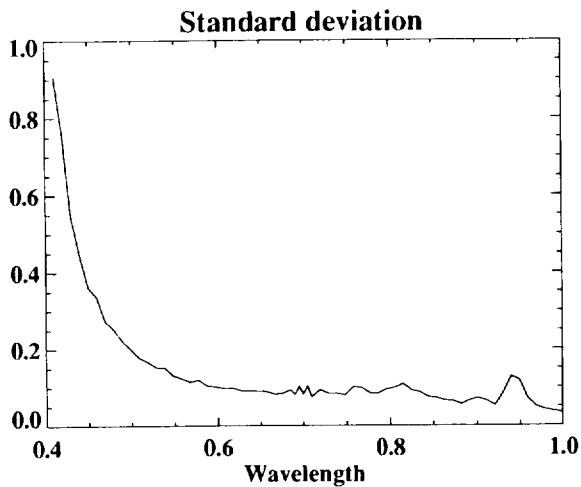


Figure 5. Standard deviation of 2000 pixels over clear water [equivalent to the in-flight noise equivalent delta radiance (NE δ L)], signal-to-noise ratio from the same data, and the calculated increase in S/N by spatially resampling AVIRIS data to 1.13 km pixels, equivalent to SeaWiFS specifications.

of Clark et al. (1988), we assumed that water depth could be estimated with an empirical model of the form

$$Z = a_0 + a_1(R_{RS\lambda 1}) + a_2(R_{RS\lambda 2}), \quad (9)$$

where R_{RS} is remotely sensed reflectance, computed from the radiance image by dividing by the LOWTRAN-modeled surface irradiance spectrum, which was resampled to AVIRIS channel responses. This assumes a constant bottom reflectance, so that bathymetry predicted in this manner, combined with in-water upwelling attenuation profiles, can be used to remove the effects of light reflected off a shallow bottom.

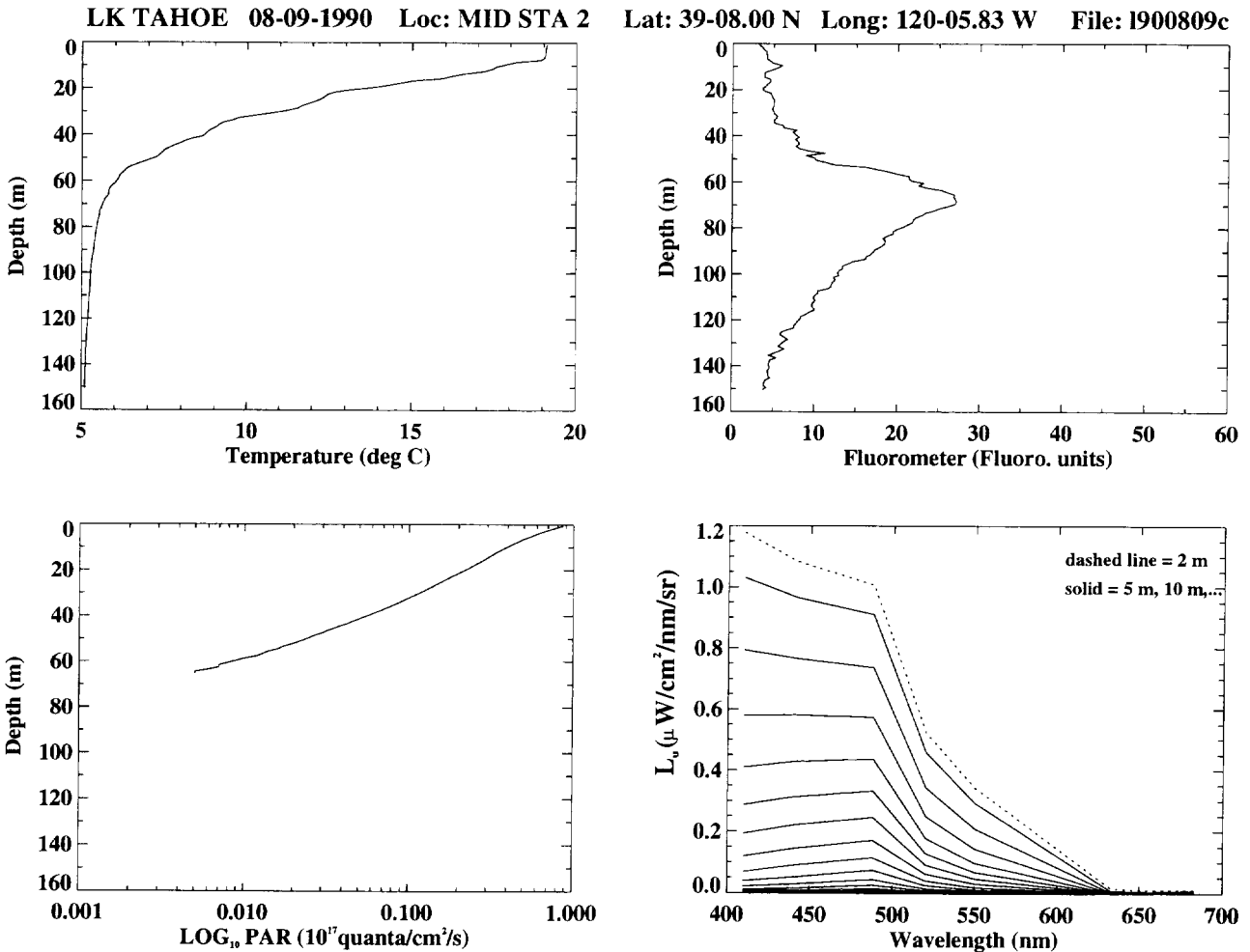
Examination of the surface reflectance spectra (Fig. 4) allowed the choosing of two wavelengths where high variability indicated the instruments response to the changing amount of light reflected off the bottom of the lake, 490 nm and 560 nm.

A multiple regression was performed to condition the model and solve for the linear coefficients, which were found to be $a_0 = 34.96$, $a_1 = 23.36$, and $a_2 = 34.64$, with a multiple correlation coefficient of 0.96. Using those results, a 200×200 pixel subscene with clearly varying water depth was selected to test the algorithm, and a simple 2×2 pixel binning was performed to increase the signal-to-noise ratio. Application of the algorithm to the image then yielded a depth estimate for each 40 m pixel.

RESULTS AND DISCUSSION

Increasing the SNR in the blue end of the spectrum is necessary to use AVIRIS data for quantitative determination of photosynthetic pigment.

Figure 6. Temperature, chlorophyll fluorescence, photosynthetically available radiation, and upwelling spectral radiance measured with the biooptical profiling system.



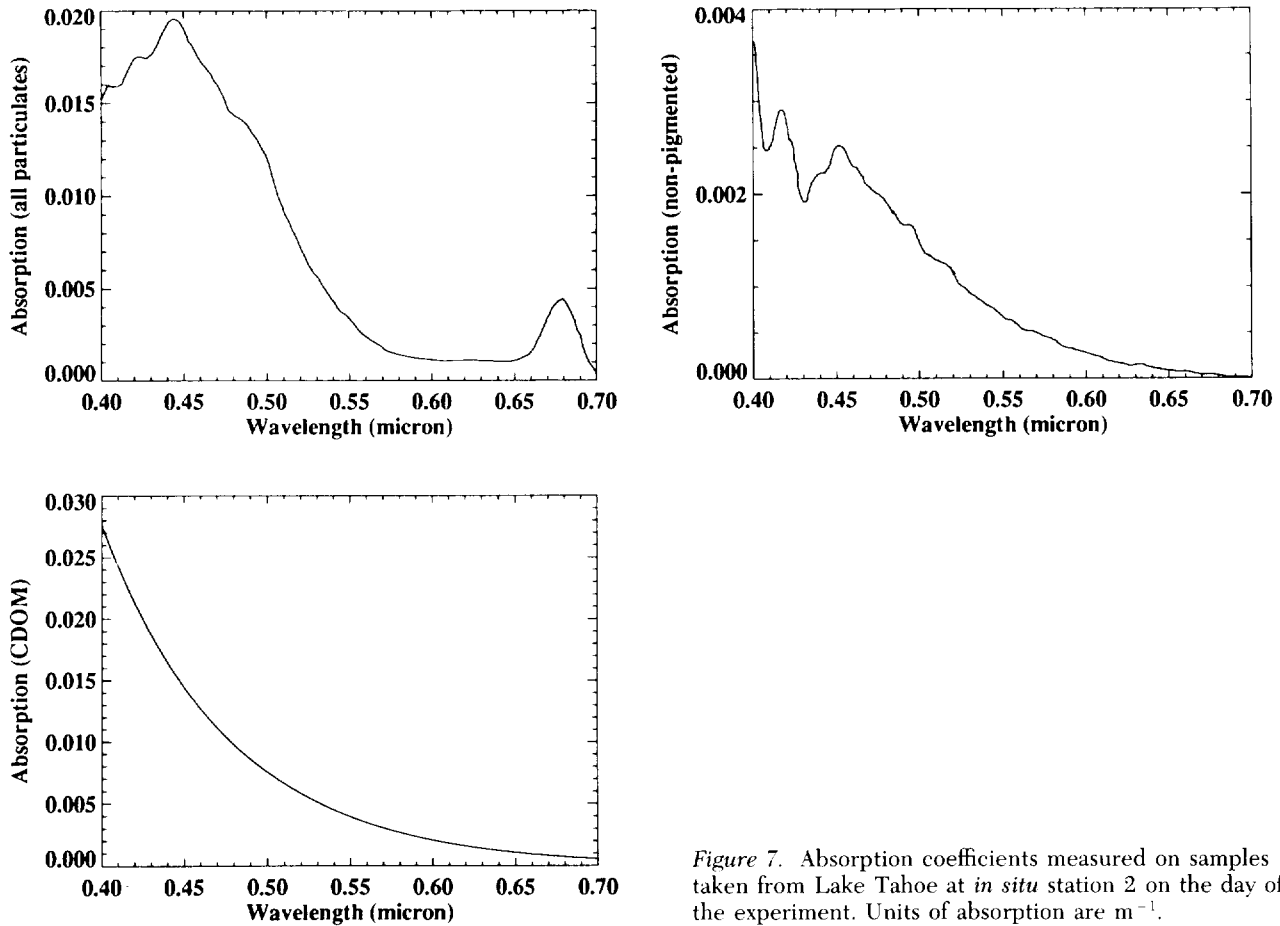


Figure 7. Absorption coefficients measured on samples taken from Lake Tahoe at *in situ* station 2 on the day of the experiment. Units of absorption are m^{-1} .

Two approaches were used to achieve this goal. First, the spectral filtering algorithm removes spurious periodicities while minimizing the loss of signal. Second, spatially resampling the image to a 1.13 km pixel size increases the signal-to-noise ratio by a factor of approximately 25, exceeding SeaWiFS specifications (Fig. 5) and bringing it into the projected sensitivity of MODIS-N.

The temperature profile (Fig. 6) indicates a well-mixed upper 10 m, with a broad thermocline between 10 m and 65 m. Chlorophyll fluorescence has a maximum at the base of the thermocline, which is indicative of a population of phytoplankton that are supported by a diffusion nutrient flux from below. Percent transmission of light is high (>90% at 660 nm; not shown) and is nearly uniform with depth with a small minimum at the base of the thermocline, again caused by the phytoplankton and detritus found there. PAR is attenuated with no significant deviations from the

characteristic logarithmic profile that is to be expected from pure water (e.g., Smith and Baker, 1978).

Spectral absorption coefficients for pigments, particulates, and CDOM are shown in Figure 7. The shape of the particulate absorption spectrum indicates the presence of chlorophyll; however, the magnitude of the absorption coefficient near 440 nm ($\sim 0.02 \text{ m}^{-1}$), as well as the lack of a reduction in the upwelling radiance (L_u , Fig. 6) at the same wavelength implies a very low concentration. This has been verified with bottle samples; concentration of chlorophyll in the surface waters at station 2 was 0.16 mg m^{-1} , of the order expected in the oligotrophic ocean (for example, the central gyre of the North Pacific basin or the Sargasso Sea).

Figure 8 illustrates the performance of the instrument over a dark body of water. In-water measurements of upwelling radiance, transformed

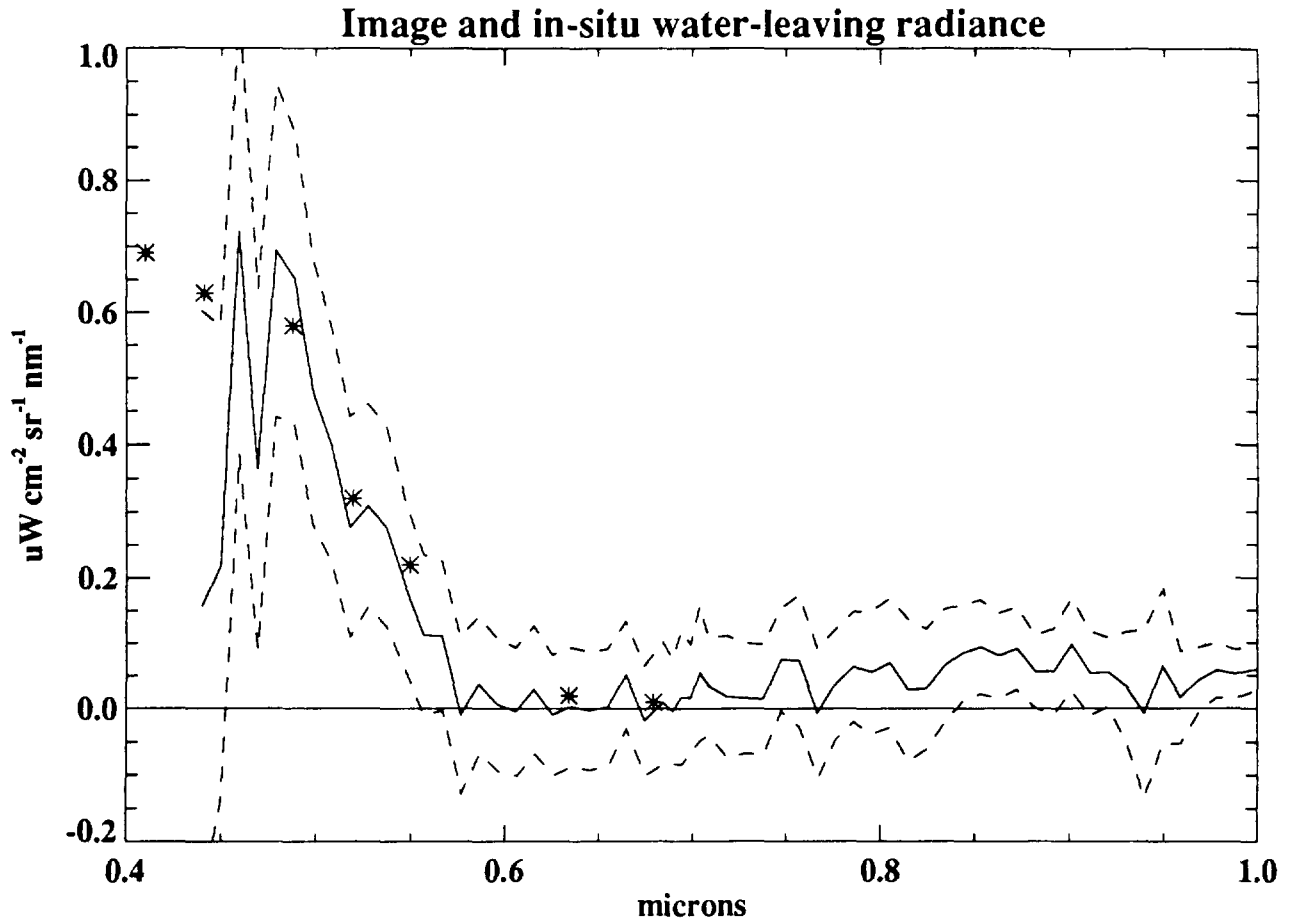


Figure 8. Comparison of the water-leaving radiance measured using the AVIRIS, and the same quantity derived by propagating in-water measurements to just above the surface (discrete points).

to water-leaving radiance, compare extremely well with image L_w at wavelengths longer than 480 nm. In the shorter wavelengths, the 1990 instrument calibration is of insufficient sensitivity to resolve a target that reflects almost no light. To overcome this limitation, Carder et al. (1993) have developed a recalibration scheme which uses *in situ* measurements of surface reflectance (transformed to water-leaving radiance) to adjust the calibration coefficients supplied by the AVIRIS project. This technique brings the image into compliance with the *in situ* measurements, but was not performed as a part of this study. Instead, L_w from the in-water measurements was substituted for L_w derived from the image, to derive estimates of pigment concentration. The ratio of $L_w440(\text{BOPS})$ to $L_w440(\text{image})$ from the station occupied at the time of the overflight was applied to the remainder of the image, in order to correct for the apparent calibration problem. This is equiv-

alent to the technique of Carder et al. (1993), but recalibrating only the channel necessary for the pigment model.

Using the low-pigment variant of the CZCS algorithm (Gordon et al., 1983) with this adjustment to L_w440 , an image representing surface chlorophyll concentration was derived. As expected, no significant variability in pigment features was seen. The average chlorophyll value for the portion of the scene where sampling station 3 was located was estimated by the case 1 algorithm to be 0.144 mg m^{-3} , very close to the bottle measurement of 0.16 mg m^{-3} . The general shape of the in-water spectrum (Fig. 6), with a lack of absorption at 410 nm, shows that the station where the profile was collected had little CDOM to obfuscate the results of the pigment model. Application of the case 1 algorithm to the remaining lake area generates poor results, due to covarying absorption by CDOM at 410 nm and

440 nm. Other stations occupied on the lake showed absorption at 410 nm (figure not shown). A model has been developed (Carder et al., 1991), which takes this into account and estimates the contribution of absorption by CDOM; however, in an area of very low concentration of chlorophyll combined with a relatively high level of degradation products, the model is extremely sensitive and gives large differences in results with small changes in parameters. Further, the algorithm requires accurate $L_w 410$, necessitating a complete recalibration of the image.

Bathymetry estimated from AVIRIS radiance measurements is shown in Figure 9, along with the NOAA bathymetry map over the same area. While not identical, the derived depth estimates do compare well in that the major features are reproduced, including the depth of the slope-break at ~ 60 ft. Because the model was conditioned in no more than 10.4 m (35 ft) of water, the estimated bathymetry loses accuracy in the deeper portion of the subscene. Use of AVIRIS to estimate shallow bathymetry appears promising and worthy of future investigation. Given a fairly constant bottom reflectance in a shallow coastal region, a day of surface measurements along with an AVIRIS overflight can be used to characterize a coastal area, in terms of the additional radiance received by the sensor that is due solely to the effects of the bottom. Conversely, in very shallow or clear waters the spectral information in AVIRIS data can be used to identify benthic algae, kelp beds, or other bottom types which have strong spectral signatures, if bottom reflectance is not constant.

SUMMARY AND CONCLUSIONS

Atmospherically corrected spectral radiance measured using AVIRIS agrees well with upwelling radiance derived from in-water spectral measurements, over an inland lake with clear water. Values of chlorophyll concentration, calculated using a variant of the CZCS case 1 algorithm with the AVIRIS image and checked with both bottle samples and in-water measurements of upwelling radiance agree quite well. This is in contrast to eutrophic bodies of water with high concentrations of pigment, where the signal received by the sensor is insufficient in the bands pertinent to

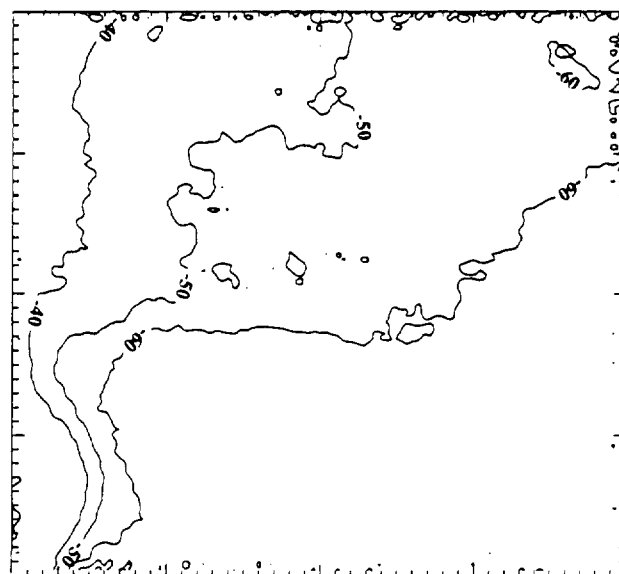
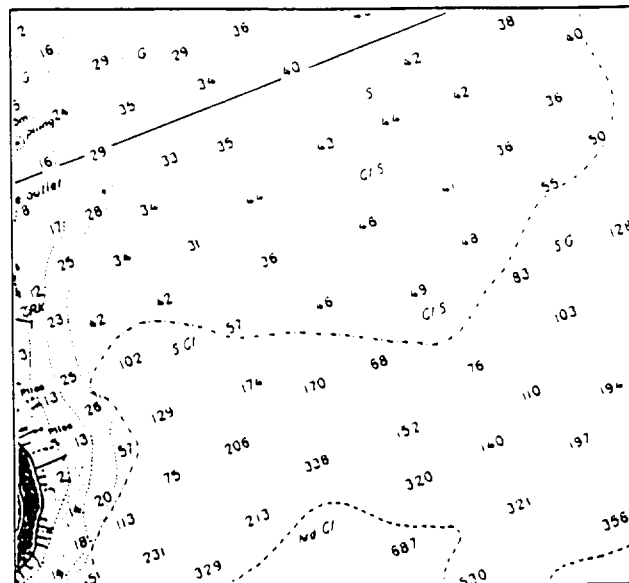


Figure 9. A contour map of modeled bathymetry, and a portion of the published soundings of the lake. Depth is in feet, for comparison to the sounding chart, but transect distance is in meters ($40 \text{ m} = 1 \text{ } 2 \times 2 \text{ binned pixel} = 1 \text{ tick mark}$).

absorption by chlorophyll to make good estimates (e.g., Melack and Pilorz, 1990). AVIRIS data quality has risen to the point where it is now useful in estimating low pigment concentrations in oligotrophic waters. Bathymetry derived from empirical modeling compares well with published lake soundings, and shows promise as a technique for characterizing coastal areas for the purpose of

removing bottom effects from remotely-sensed color imagery.

AVIRIS is useful for a variety of oceanographic and limnologic applications, and algorithm development is underway to standardize techniques that have been previously published, and derive and test new ones.

The authors thank the AVIRIS engineering team for their continuing efforts to improve the performance of the instrument. We thank the AVIRIS operations team and the NASA Ames Research Center, High Altitude Branch for collecting the AVIRIS data. John Melack (U.C., Santa Barbara) organized the field work and Robert Richards (U.C., Davis) provided the ship support. Jeannette van den Bosch, Curt Mobley, Joan Cleveland, and Joshua Mertz provided valuable comments and editing assistance. This work was carried out at the Jet Propulsion Laboratory, California Institute of Technology, and at the University of South Florida, and was supported by contracts from the National Aeronautics and Space Administration to those institutions. Reference herein to any specific commercial product, process, or service by trade name, trademark, manufacturer, or otherwise, does not constitute or imply its endorsement by the United States Government, the Jet Propulsion Laboratory, California Institute of Technology, or the University of South Florida.

REFERENCES

- Austin, R. W. (1974), The remote-sensing of spectral radiance from below the ocean surface, in *Optical Aspects of Oceanography* (N. G. Jerlov and E. Steeman Nielsen, Eds.), Academic, London, pp. 317-344.
- Baker, J., and Ruggles, K. W. (1987), System concept for wide-field-of-view observations of ocean phenomena from space, Report of the Joint EOSAT/NASA Working Group, Earth Observation Satellite Co., Lanham, MD, 92 pp.
- Boardman, J., and Goetz, A. F. H. (1991), Sedimentary facies analysis using AVIRIS data: a Geophysical Inverse Problem, in *Proceedings of the Third Airborne Visible / Infrared Imaging Spectrometer Workshop*, JPL Publication 91-28, Pasadena, CA, pp. 4-13.
- Bricaud, A., Bedhomme, A.-L., and Morel, A. (1988), Optical properties of diverse phytoplanktonic species: Experimental results and theoretical interpretation, *J. Plankton Res.* 10:851-873.
- Carder, K. L., and Steward, R. G. (1985), A remote-sensing reflectance model of a red tide dinoflagellate off West Florida, *Limnol. Oceanogr.* 30:286-298.
- Carder, K. L., Hawes, S. K., Baker, S. K., Smith, R. C., Steward, R. G., and Mitchell, B. G. (1991), Reflectance model for quantifying chlorophyll-*a* in the presence of productivity degradation products, *J. Geophys. Res.* 96 (C11): 20,599-20,611.
- Carder, K. L., Reinersman, P., Chen, R. F., Davis, C. O., and Hamilton, M. (1993), AVIRIS calibration and application in coastal oceanic environments, *Remote Sens. Environ.* 44:205-216.
- Clark, R. N., Faye, T. H., and Walker, C. L. (1988), Bathymetry using Thematic Mapper Imagery, in: *Ocean Optics IX* (Richard W. Spinrad, Ed.), Proc. SPIE 925, pp. 229-231.
- Goetz, A. F. H., and Davis, C. O. (1991), High Resolution Imaging Spectrometer (HIRIS): science and instrument, *Int. J. Imaging Syst. Technol.* 3:131-143.
- Gordon, H., Clark, D., Brown, J., Brown, O., Evans, R., and Brokenow, W. (1983), Phytoplankton pigment concentrations in the Middle Atlantic Bight: comparison of ship determinations and CZCS estimates, *Appl. Opt.* 22(1): 20-36.
- Gordon, H., Brown, O., Evans, R., et al. (1988), Semianalytic radiance model of ocean color, *J. Geophys. Res.* 93(D9): 10,909-10,924.
- Green, R. O., Conel, J. E., Margolis, J. S., Bruegge, C. J., and Hoover, G. L. (1991), An inversion algorithm for retrieval of atmospheric and leaf water absorption from AVIRIS radiance with compensation for atmospheric scattering, in *Proceedings of the Third Airborne Visible / Infrared Imaging Spectrometer (AVIRIS) Workshop*, Robert Green, ed., JPL Publication 91-28, Pasadena, CA, pp. 51-61.
- Hovis, W. A., Clark, D. K., Anderson, F., et al. (1980), Nimbus-7 coastal zone color scanner; system description and initial imagery. *Science* 210:60-63.
- Kiefer, D. A., and Soohoo, J. B. (1982), Spectral absorption by marine particles of coastal water of Baja, California, *Limnol. Oceanogr.* 27:492-499.
- Kirk, J. T. O. (1976), Yellow Substance (Gelbstoff) and its contribution to the attenuation of photosynthetically active radiation in some inland and coastal southeastern Australian waters, *Aust. J. Mar. Freshwater Res.* 27:61-71.
- Kishino, M., Takahashi, M., Okami, N., and Ichimura, S. (1985), Estimation of spectral absorption coefficients of phytoplankton in the sea, *Bull. Mar. Sci.* 37(2):634-642.
- Kneizys, F. X., Shettle, E. P., Abreu, L. W., et al. (1988), *Users Guide to LOWTRAN 7*, Air Force Geophysical Laboratory, AFGL-TR-88-0177, Environmental Research Papers, No. 1010.
- Melack, J., and Pilorz, S. H. (1990), Reflectance spectra from eutrophic Mono Lake, California, measured with the Airborne Visible and Infrared Imaging Spectrometer (AVIRIS), in *Proceedings of the Second Airborne Visible and Infrared Imaging Spectrometer Workshop*, JPL Publication 90-54, Pasadena, CA, pp. 232-242.
- Mitchell, B. G., and Kiefer, D. A. (1988), Variability in pigment-specific particulate fluorescence and absorption spectra in the NE Pacific Ocean, *Deep Sea Res.* 35(5): 665-689.
- Morel, A. (1988), Optical Modeling of the upper ocean in

- relation to its biogenous matter content (Case I waters), *J. Geophys. Res.* 93(C9):10,749–10,768.
- Peacock, T. P., Carder, K. L., Davis, C. O., and Steward, R. G. (1990), Effects of fluorescence and Raman scattering on models of remote-sensing reflectance, in *Ocean Optics X*, Proc. SPIE, 1302, Intl. Soc. Optical Eng., Bellingham, WA, pp. 303–319.
- Pilorz, S. H., and Davis, C. O. (1990a), Investigations of Ocean Reflectance with AVIRIS data, in *Proceedings of the Second Airborne Visible / Infrared Imaging Spectrometer Workshop*, JPL Publication 90-54, Pasadena, CA, pp. 224–231.
- Pilorz, S. H., and Davis, C. O. (1990b), Spectral Decomposition of sea surface reflected radiance, in *Proceedings, IGARSS 1990 (1)*, IEEE, New York, pp. 345–348.
- Rast, M., and Bezy, J. L. (1990), ESA's Medium Resolution Imaging Spectrometer: mission, system and applications, in *Proc. SPIE 1298, Imaging Spectroscopy of the Terrestrial Environment*, Intl. Soc. Optical Eng., Bellingham, WA, pp. 114–126.
- Roesler, C. S., Perry, M. J., and Carder, K. L. (1989), Modeling *in situ* phytoplankton absorption from total absorption spectra, *Limnol. Oceanogr.* 34(8):1510–1523.
- Salmonson, V., Barnes, B., Maymon, P. W., Montgomery, H., and Ostrow, H. (1989), MODIS: advanced facility instrument for the study of the Earth as a system, *IEEE Trans. Geosci. Remote Sens.* GE-27:145–153.
- Smith, R. C., and Baker, K. (1978), Optical classification of natural waters, *Limnol. Oceanogr.* 23:260–267.
- Smith, R. C., Booth, C. R., and Star, J. L. (1984), Oceanographic bio-optical profiling system, *Appl. Opt.* 23:2791–2797.
- Strickland, J. D. H., and Parsons, T. R. (1972), A practical handbook of seawater analysis, *Fish. Res. Bd. Canada Bull.* 167, 311 pp.
- van den Bosch, J. M., and Alley R. (1990), Application of LOWTRAN 7 as an atmospheric correction to airborne visible / infrared imaging spectrometer (AVIRIS) data, in *Proceedings of the Second Airborne Visible and Infrared Imaging Spectrometer Workshop*, JPL Publication 90-54, Pasadena, CA, pp. 78–81.
- Vane, G., Green, R. O., Chrien, T. G., Enmark, H. T., Hansen, E. G., and Porter, W. M. (1993), The airborne visible / infrared imaging spectrometer (AVIRIS), *Remote Sens. Environ.* 44:127–143.
- Yoder, J. A., and Fukushima, H. (1991), Satellite ocean color, in *Proceedings of a Joint US-Japan Seminar Program*, East-West Center, Honolulu, Hawaii, 7–10 May, 27 pp, plus appendix.